Opal–AgI photonic crystal controlled by the superionic phase transition

6 AUTHORS, INCLUDING:

Dmitry Kurdyukov

Ioffe Physical Technical Institute

139 PUBLICATIONS **1,358** CITATIONS

Valery Grigorievich Golubev

Ioffe Physical Technical Institute

176 PUBLICATIONS **1,293** CITATIONS

Opal–AgI photonic crystal controlled
by the superionic phase transition

Alexander V. Il'inskii[1], **Rasul A. Aliev**[2], **Dmitry A. Kurdyukov**[*, 2],
Nataliya V. Sharenkova[2], **Evgenii B. Shadrin**[2], and **Valery G. Golubev**[2]

[1] Behemérita Universidad Autóhoma de Puebla, Puebla, 72000 Pue, Mexico
[2] Ioffe Physico-Technical Institute, Russian Academy of Sciences, 26 Politekhnicheskaya,
St. Petersburg 194021, Russia

A three-dimensional photonic crystal based on an opal–AgI composite was fabricated using a high-pressure melt technique. It is shown that the semiconductor–superionic conductor phase transition in AgI controls electronic and optical properties of the composite.

1 Introduction

Synthetic opal is a good example of a three-dimensional (3D) photonic crystal having an fcc lattice composed of close-packed monodisperse $a\text{-}SiO_2$ spheres with a diameter varying within 200–1000 nm [1]. Optical and photonic band gap (PBG) properties of opals may be changed by varying both the size of the spheres and controllable filling of the interconnected opal pores with various fillers [2]. Many potential applications require using special methods to govern the PBG structure of photonic crystals in real time under external effects. Numerous principles of external control of the PBG in 3D opal-based photonic crystals, like applying an external electric field [3–7], optical excitation [8–14], and temperature variation [15–19], have been proposed and tested experimentally.

Silver iodide (AgI) is a polymorphic material where several different solid phases exist: γ, β, and α in order of increasing temperature. At temperatures higher than the superionic transition point T_c, the semiconductor β phase with a hexagonal wurtzite structure undergoes a first-order phase transition and transforms into the superionic conductor α phase [20]. $\alpha\text{-}AgI$, which is known as one of the best superionic conductors, has a bcc cubic arrangement of I^- anions with highly mobile Ag^+ cations randomly distributed and hopping through the tetrahedral interstices. It is also well known that many of the physical properties of AgI (conductivity, dielectric constants, etc.) change at T_c.

Our work shows that an opal–AgI composite is a challenging material for creating a controllable photonic crystal.

2 Experimental results and discussion

We used synthetic opals formed from close-packed monodisperse 230 ± 5 nm diameter $a\text{-}SiO_2$ spheres that have the fcc lattice as a template for impregnation of silver iodide. The opals had a regular interconnected sublattice of pores occupying about 26% from the whole sample volume. The bare opals have

* Corresponding author: e-mail: kurd@gvg.ioffe.ru, Phone: +7 812 247 93 93, Fax: +7 812 247 10 17
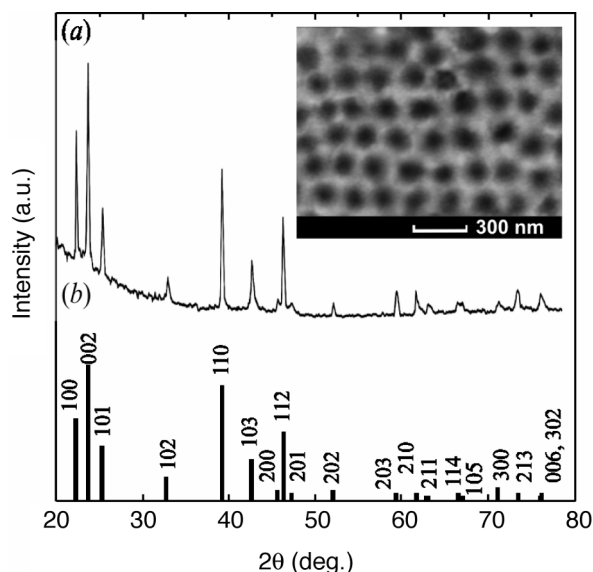
Fig. 1 X-ray diffraction patterns of a) the opal–AgI composite and b) the bulk AgI sample. Inset shows FESEM micrograph of the polished opal–AgI composite.

been grown by use of the technological route described in Ref. [21]. The opal templates had polydomain structure. The size of a single domain with highly ordered SiO_2 spheres ranged from 30 to 100 μm.

The experimental samples were $4 \times 4 \times 0.5$ mm^3 plates cut parallel to the (111) opal plane. The opal pores were filled with AgI melt at $T = 600$ °C by a high-pressure technique similar to that described in Ref. [22]. The technique provided for complete and uniform filling of the pores with AgI throughout the whole sample. Then, the surface of the AgI-infiltrated opals was mechanically polished to remove an AgI film from the surface of the samples. For the polishing we used a diamond powder with grain size <1 μm. The gravimetric density (ρ) of the polished samples was found to be 2.7 g/cm^3. The filling factor was calculated as

$$\frac{\rho - \rho_0}{0.26\rho_{AgI}} \times 100\% = 94\% \,,$$

where $\rho_{AgI} = 5.7$ g/cm^3 and $\rho_0 = 1.3$ g/cm^3 are the gravimetric densities of bulk AgI and bare opal, correspondingly. The inaccuracy in the filling factor measurements did not exceed 5% [23]; therefore, the opal pores were almost completely filled with silver iodide. Then, the opal–AgI samples were checked by a field-emission scanning electron microscope (FESEM), and the best samples were selected for the optical measurements.

The opal–AgI composite was studied by an X-ray diffraction (XRD) method at room temperature using a DRON-2 diffractometer. The XRD pattern presented in Fig. 1 shows that the composite does not contain other crystalline phases except for β-AgI. Some differences in the intensity ratios of the diffraction maxima in the opal–AgI spectrum (Fig. 1a) compared with those in bulk AgI (Fig. 1b) are due to the preferred texture growth of AgI crystallites in the opal pores. The determined lattice parameters of AgI inside the opal pores ($a_o = 4.591(3)$ Å, $c_o = 7.499(7)$ Å) are in good agreement with the values for bulk AgI [24]. The inset in Fig. 1 shows a FESEM image of the surface of the opal–AgI composite. It demonstrates the regular crystalline structure of close-packed spheres in the (111) plane. Practically all pores were uniformly impregnated with a substance. Such a conclusion is being drawn on the basis of comparing the contrast of the silica sphere and the area which before the infiltration process was an octahedral (tetrahedral) void. Since the contrast depends on secondary electron emission, the silica spheres look darker than the filler between them.
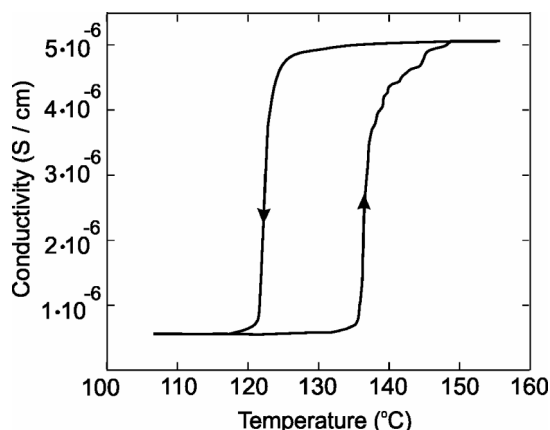
Fig. 2 Thermal hysteresis loop of the opal–AgI composite conductivity.

Figure 2 demonstrates that at temperatures as high as 135 °C a transition of the material into a high-mobility superionic state arises. The abrupt increase in conductivity is due to a reversible phase transition from the β to the α phase following extensive Ag^+ disorder and greatly enhanced Ag^+ conductivity. The highly conducting (fast-ionic) state is achieved due to stepwise growth in concentration of Frenkel defects as a result of the β → α-AgI first-order structural phase transition. A rapid increase in concentration of Frenkel defects is explained by a temperature-dependent decrease in the Gibbs free energy for defect formation [25].

Note that while the temperature increases the formation of germs of high-conducting phase in the opal−AgI composites occurs in regularly located regions of space (ordered opal pores). This complicates the formation of an infinite conducting cluster, contrary to AgI films. In the films where the material has a phase transition, the infinite conducting cluster is formed from irregularly located conducting chains [26]. Therefore, the temperature rise of the heating branch at the hysteresis loop of conductivity (Fig. 2) in the ordered opal−AgI composite occurs more abruptly and at higher T_c than in the films. The reason for this is that the phase transition takes place simultaneously in almost all germs located within the ordered opal pores.

The abrupt fall of conductivity in the cooling branch of the hysteresis loop (Fig. 2) occurs at the temperature corresponding to the destruction of the infinite conducting cluster. Therefore, the temperature slope of the cooling branch is nearly vertical, similar to the heating branch.

To study optical and PBG properties of the synthesized composites, we measured specular reflection spectra from the (111) lattice planes of the opal–AgI composite and the bare opal (Fig. 3). To avoid any contribution of the opal polydomain structure and structural defects to the signal being measured, we used the so-called light microscopic technique [27]. The Bragg reflection maximum λ_{111} obeys Snell's formula $\lambda_{111} = 2d_{(111)}\sqrt{\langle\varepsilon\rangle - \sin^2\theta}$, where θ is the angle of light incidence, $d_{(111)}$ is the interplane distance in the fcc lattice of the composite in the [111] direction, and $\langle\varepsilon\rangle$ is the average dielectric constant of the composite; $\langle\varepsilon\rangle = \sum \varepsilon_i f_i$ [17, 28−31], where ε_i and f_i are the dielectric constant and the volume fraction of the *i*-th component of the composite, respectively. One can see the long-wavelength shift of the Bragg reflection maximum λ_{111} (curves 1, 2 in Fig. 3) by about 115 nm caused by infiltration of the opal pores with AgI, and a corresponding increase of $\langle\varepsilon\rangle$ from 1.670 to 2.538. The calculated dielectric constant of AgI inside the opal pores (we used a filling factor value equal to 94 vol% in the calculations) was found to be 4.57, which is in good agreement with the value for bulk AgI [20]. One can also notice that the position of the Bragg reflection λ_{111} shifts towards shorter wavelengths as the θ magnitude increases (curves 2−4 in Fig. 3). The fact of the appearance of pronounced peaks of Bragg reflections testifies to the homogeneous distribution of the guest material in the pores of the opal matrix and confirms the presence of a well-formed photonic crystal structure of the composites under study.
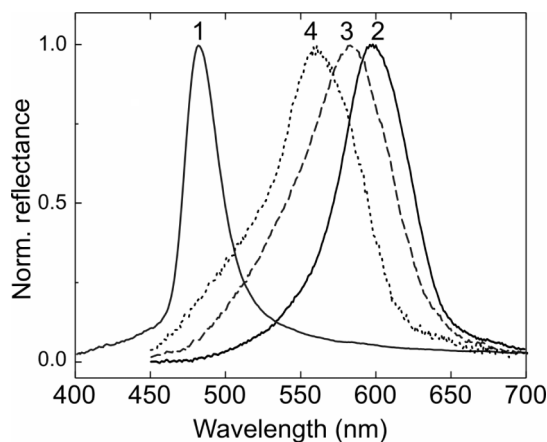
Fig. 3 Normalized spectra of reflection measured at room temperature from the (111) surface of the bare opal (1) and the opal–AgI composite (2–4). Angle of registration relative to the normal to the (111) surface of the samples: 1–0°, 2–0°, 3–30°, 4–45°.
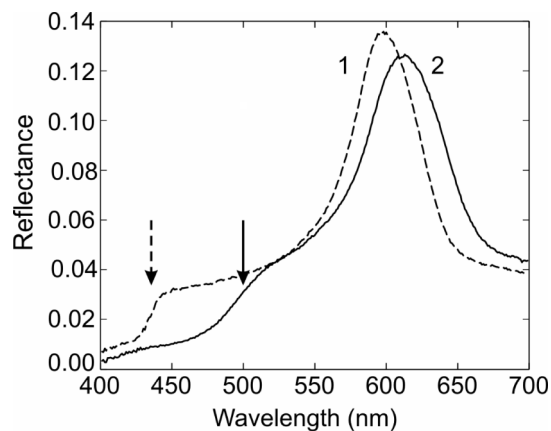
Fig. 4 Reflection spectra from the (111) surface of the opal–AgI composite: (1) AgI in the semiconductor phase, $T = 90\ °C$; (2) AgI in the superionic phase, $T = 150\ °C$.

Figure 4 presents the reflection spectra from the (111) opal–AgI composite surface at normal light incidence. The spectra were measured at two temperature values: below T_c (the semiconductor phase) and above it (the superionic phase). The observable peaks, which are due to the Bragg diffraction of electromagnetic waves by the periodic structure of the samples, characterize the PBG in the [111] direction. The sample heating leads to the phase transition in AgI, increases its dielectric constant, and finally increases the average dielectric constant from 2.538 to 2.667. As a result, the Bragg diffraction peak shifts towards the long-wave region by about 15 nm. The calculated dielectric constant of AgI inside the opal pores (94 vol%) after the phase transition was found to be 5.09.

The spectra also show terraces (see arrows in Fig. 4), which correspond to a variation of the optical absorption edge from 2.85 to 2.5 eV due to the electronic band gap narrowing under the phase transition [20]. Thermal hysteresis loops of both the Bragg peak position and the terrace were observed. The loop configuration looks like that in conductivity measurements presented in Fig. 2. Note that a good reproducibility of all spectral characteristics was observed in numerous heating-cooling cycles.

3 Conclusions

A three-dimensional photonic crystal based on an opal–AgI composite was prepared by a high-pressure melt technique. XRD confirms that a material prepared in interconnected synthetic silica opal pores is β-AgI. Conductivity and optical reflectivity measurements confirmed that optical and photonic band gap properties of the opal–AgI composite are controlled by the β → α-AgI superionic phase transition.

References

[1] Y. Xia, B. Gates, Y. Yin, and Y. Lu, Adv. Mater. **12**, 693 (2000).
[2] C. López, Adv. Mater. **15**, 1679 (2003).
[3] D. Kang, J. E. Maclennan, N. A. Clark, A. A. Zakhidov, and R. H. Baughman, Phys. Rev. Lett. **86**, 4052 (2001).

 [4] Q.-B. Meng, C.-H. Fu, S. Hayami, Z.-Z. Gu, O. Sato, and A. Fujishima, J. Appl. Phys. **89**, 5794 (2001).
 [5] Y. Shimoda, M. Ozaki, and K. Yoshino, Appl. Phys. Lett. **79**, 3627 (2001).
 [6] P. Mach, P. Wiltzius, M. Megens, D. A. Weitz, K.-H. Lin, T. C. Lubensky, and A. G. Yodh, Phys. Rev. E **65**, 031720 (2002).
 [7] B. Li, J. Zhou, L. Li, X. J. Wang, X. H. Liu, and J. Zi, Appl. Phys. Lett. **83**, 4704 (2003).
 [8] G. Pan, R. Kesavamoorthy, and S. A. Asher, Phys. Rev. Lett. **78**, 3860 (1997).
 [9] A. V. Akimov, A. V. Virchenko, V. G. Golubev, A. A. Kaplyanskii, D. A. Kurdyukov, A. B. Pevtsov, and A. V. Shcherbakov, Phys. Solid State **45**, 240 (2003).
[10] D. A. Mazurenko, R. Kerst, J. I. Dijkhuis, A. V. Akimov, V. G. Golubev, D. A. Kurdyukov, A. B. Pevtsov, and A. V. Sel'kin, Phys. Rev. Lett. **91**, 213903 (2003).
[11] X. Hu, Q. Zhang, Y. Liu, B. Cheng, and D. Zhang, Appl. Phys. Lett. **83**, 2518 (2003).
[12] D. A. Mazurenko, R. Kerst, J. I. Dijkhuis, A. V. Akimov, V. G. Golubev, A. A. Kaplyanskii, D. A. Kurdyukov, and A. B. Pevtsov, Appl. Phys. Lett. **86**, 041114 (2005).
[13] Y. Liu, X. Hu, D. Zhang, B. Cheng, D. Zhang, and Q. Meng, Appl. Phys. Lett. **86**, 151102 (2005).
[14] C. Becker, S. Linden, G. von Freymann, M. Wegener, N. Tétreault, E. Vekris, V. Kitaev, and G. A. Ozin, Appl. Phys. Lett. **87**, 091111 (2005).
[15] K. Yoshino, Y. Shimoda, Y. Kawagishi, K. Nakayama, and M. Ozaki, Appl. Phys. Lett. **75**, 932 (1999).
[16] J. Zhou, C. Q. Sun, K. Pita, Y. L. Lam, Y. Zhou, S. L. Ng, C. H. Kam, L. T. Li, and Z. L. Gui, Appl. Phys. Lett. **78**, 661 (2001).
[17] V. G. Golubev, V. Yu. Davydov, N. F. Kartenko, D. A. Kurdyukov, A. V. Medvedev, A. B. Pevtsov, A. V. Scherbakov, and E. B. Shadrin, Appl. Phys. Lett. **79**, 2127 (2001).
[18] G. Mertens, T. Röder, R. Schweins, K. Huber, and H.-S. Kitzerow, Appl. Phys. Lett. **80**, 1885 (2002).
[19] V. G. Golubev, D. A. Kurdyukov, A. B. Pevtsov, A. V. Sel'kin, E. B. Shadrin, A. V. Il'inskii, and R. Boeyink, Semiconductors **36**, 1043 (2002).
[20] K. Wakamura, Solid State Ion. **149**, 73 (2002).
[21] W. Stoeber, A. Fink, and E. Bohn, J. Colloid Interface Sci. **26**, 62 (1968).
[22] J. H. P. Watson, Phys. Rev. **148**, 223 (1966).
[23] N. A. Feoktistov, V. G. Golubev, J. L. Hutchison, D. A. Kurdyukov, A. B. Pevtsov, V. V. Ratnikov, J. Sloan, and L. M. Sorokin, Semicond. Sci. Technol. **16**, 955 (2001).
[24] W. Jos, H. Gel, and G. Schniedermann, Nat. Bur. Standards Circ. **8**, 539 (1958).
[25] M. Anija, Solid State Ion. **50**, 125 (1992).
[26] S. Havlin and A. Bunde, in: Fractals and Disordered Systems, edited by A. Bunde and S. Havlin (Springer-Verlag, Berlin, 1994), 321 pages.
[27] V. G. Golubev, V. A. Kosobukin, D. A. Kurdyukov, A. V. Medvedev, and A. B. Pevtsov, Semiconductors **35**, 680 (2001).
[28] S. G. Romanov, T. Maka, C. M. Sotomayor Torres, M. Müller, R. Zentel, D. Cassagne, J. Manzanares-Martinez, and C. Jouanin, Phys. Rev. E **63**, 056603 (2001).
[29] Y. Lin, J. Zhang, E. H. Sargent, and E. Kumacheva, Appl. Phys. Lett. **81**, 3134 (2002).
[30] H. Míguez, A. Blanco, F. Meseguer, C. López, H. M. Yates, M. E. Pemble, V. Fornés, and A. Mifsud, Phys. Rev. B **59**, 1563 (1999).
[31] J. Valenta, J. Linnros, R. Juhasz, J.-L. Rehspringer, F. Huber, C. Hirlimann, S. Cheylan, and R. G. Elliman, J. Appl. Phys. **93**, 4471 (2003).